Quantum Phase Transition and Emergent Symmetry in a Quadruple Quantum Dot System

Dong E. Liu, Shailesh Chandrasekharan, and Harold U. Baranger

Department of Physics, Duke University, Box 90305, Durham, North Carolina 27708-0305, USA

(Received 6 August 2010; published 13 December 2010)

We propose a system of four quantum dots designed to study the competition between three types of interactions: Heisenberg, Kondo, and Ising. We find a rich phase diagram containing two sharp features: a quantum phase transition (QPT) between charge-ordered and charge-liquid phases and a dramatic resonance in the charge liquid visible in the conductance. The QPT is of the Kosterlitz-Thouless type with a discontinuous jump in the conductance at the transition. We connect the resonance phenomenon with the degeneracy of three levels in the isolated quadruple dot and argue that this leads to a Kondo-like emergent symmetry from left-right Z_2 to $U(1)$.

DOI: 10.1103/PhysRevLett.105.256801 PACS numbers: 73.21.La, 05.30.Rt, 72.10.Fk, 73.23.Hk

Strong electronic correlations create a variety of interesting phenomena including quantum phase transitions [1], emergence of new symmetries [2], and Kondo resonances [3]. It is likely that new, yet undiscovered, phenomena can arise from unexplored competing interactions. Today, quantum dots provide controlled and tunable experimental quantum systems to study strong correlation effects. Further, unlike most materials, quantum dots can be modeled using impurity models that can be treated theoretically much more easily. Single quantum dots have been studied extensively, both theoretically and experimentally, which has led to a firm understanding of their Kondo physics [4,5]. More recently, the focus has shifted to multiple quantum dot systems where a richer variety of quantum phenomena become accessible [4,5]. These include emergent symmetries (the symmetry of the low energy physics is larger than the symmetry of the Hamiltonian) [6] and quantum phase transitions [7–9].

In this work we propose a quadruple quantum dot system, that is experimentally realizable, in which three competing interactions determine the low temperature physics: (1) Kondo-like coupling of each dot with its lead, (2) Heisenberg coupling between the dots, and (3) Ising coupling between the dots. Thus, there are two dimensionless parameters with which to tune the competition. The pairwise competing interactions, Kondo-Heisenberg and Kondo-Ising, have both been studied previously. The two impurity Kondo model with a Heisenberg interaction between the impurities shows an impurity quantum phase transition (QPT) from separate Kondo screening of the two spins at small exchange to a local spin singlet (LSS) phase at large exchange. This has received extensive theoretical [7,10,11] and experimental [5] attention. The competition between Kondo and Ising couplings has also been studied theoretically for two impurities [8], including in the quantum dot context [8,9]; however, no experimentally possible realization of this competition has been proposed to date.

Our system consists of four quantum dots and four leads, as shown in Fig. 1(a), with two polarized (spinless) electrons on the four dots. We find that the system has a rich phase diagram, Fig. 1(b), in terms of the strength of the Heisenberg interaction controlled by t and the Ising interaction controlled by U'. In the absence of the Ising interaction we start in the LSS phase. Upon increasing the Ising

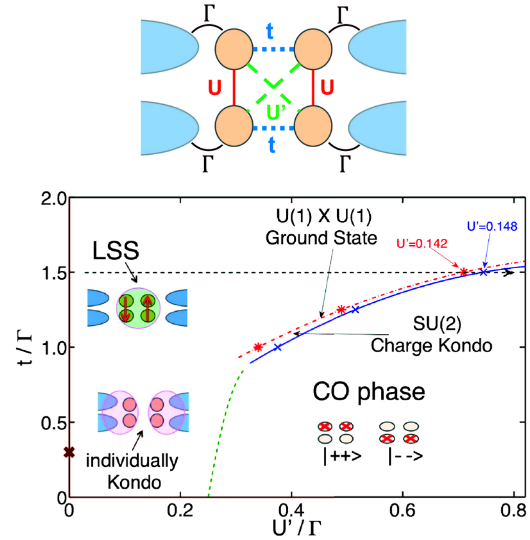

FIG. 1 (color online). (a) Quadruple-dot system. U and U' are electrostatic interactions while t and Γ involve electron tunneling. (b) Ground state phase diagram as a function of the Ising-Kondo tuning U'/Γ and the Heisenberg-Kondo tuning t/Γ, where $U = 3.0$ and $\Gamma = 0.2$. Two distinct phases—charge ordered (CO) and charge liquid—are separated by a KT quantum phase transition [blue crosses (numerical) and green dashed line (schematic)]. Several crossovers lie within the charge-liquid phase. Red stars mark the level crossing where the $U(1) \times U(1)$ state is found (numerical). The charge Kondo region lies between the red and blue lines. "LSS" denotes the local spin singlet state (Heisenberg coupling dominates), while when both Heisenberg and Ising couplings are weak, the system consists of individually screened Kondo states on the left and right. The black dashed line with arrow shows where the calculations for Figs. 2 and 3 have been done.

 © 2010 The American Physical Society

strength, we find that the system first evolves continuously to a new Kondo-type state with a novel $U(1) \times U(1)$ strong-coupling fixed point, where the symmetry of the low energy physics enhances from left-right Z_2 to $U(1)$. Then there is a crossover to a $SU(2)$ charge Kondo state. Finally, an additional small increase in U' causes a QPT of the Kosterlitz-Thouless (KT) type to a charge-ordered state (CO) (as in Refs. [8,9]) consisting of an unscreened doubly degenerate ground state [12].

Model.—The quantum dots in Fig. 1(a) are capacitively coupled in two ways: U is the vertical interaction (between $L+$ and $L-$; $R+$ and $R-$) and U' is along the diagonal (between $L+$ and $R-$; $L-$ and $R+$). Along the horizontal, there is no capacitive coupling, but there is direct tunneling t (between $L+$ and $R+$; $L-$ and $R-$). Each dot couples to a conduction lead through $\Gamma = \pi V^2 \rho$ where ρ is the density of states of the leads at the Fermi energy. The whole system is spinless. We consider only the regime in which the four dots contain two electrons.

The system Hamiltonian is $H = H_{\rm lead} + H_{\rm imp} + H_{\rm coup}$, where $H_{\rm lead} = \sum_{i,s,k} \epsilon_k c^\dagger_{isk} c_{isk}$ describes the four conduction leads ($i = L, R$; $s = +, -$), and $H_{\rm coup} = V \sum_{i,s,k} (c^\dagger_{isk} d_{is} + \text{H.c.})$ describes the coupling of the leads to the dots which produces the Kondo interaction. $H_{\rm imp}$ is the Anderson-type Hamiltonian

$$H_{\rm imp} = \sum_{i=L,R} \sum_{s=+,-} \epsilon_d d^\dagger_{is} d_{is} + \sum_{i=L,R} U \hat{n}_{i+} \hat{n}_{i-} + U'(\hat{n}_{L+}\hat{n}_{R-} + \hat{n}_{L-}\hat{n}_{R+}) + t \sum_{s=+,-} (d^\dagger_{Ls} d_{Rs} + d^\dagger_{Rs} d_{Ls}). \quad (1)$$

We take $U \gg U'$ so that there is one electron on the left and one on the right.

We can reformulate $H_{\rm imp}$ as an exchange Hamiltonian by noticing that the right-hand (left-hand) sites form a pseudospin: $\vec{S}_i = \sum_{s,s'} d^\dagger_{si} \vec{\sigma}_{ss'} d_{si}/2$. When $t \ll U$, the effective Hamiltonian for the quantum dots is

$$H^{\rm eff}_{\rm imp} \simeq J_H \vec{S}_L \cdot \vec{S}_R - \tilde{J}_z S^z_L S^z_R, \quad (2)$$

where $J_H \simeq 4t^2/(U - U'/2)$ and $\tilde{J}_z \simeq 2U'$. Thus t controls the strength of the Heisenberg interaction among the dots, and U' controls the Ising coupling. The eigenstates of the impurity site are the usual (pseudo)spin singlet and triplet states, $|S\rangle$, $|++\rangle$, $|--\rangle$, and $|T0\rangle$.

Two limits of our model have been studied previously. First, for $U' = 0$, it becomes the well-known two impurity Kondo model [10,11]. If direct charge transfer is totally suppressed, a QPT occurs between a Kondo screened state (in which the impurities fluctuate between all four states, singlet and triplet) and a LSS [10,11]. When direct tunneling is introduced, the QPT is replaced by a smooth crossover [11]. Second, when $t = 0$, the model has [8,9] a KT-type QPT between the Kondo screened phase at small U' and a CO phase at large U'. The CO phase has an unscreened doubly degenerate ground state corresponding to $|++\rangle$ and $|--\rangle$.

We solve the model (1) exactly by using finite-temperature world line quantum Monte Carlo (QMC) simulation with directed loop updates [13,14]. We study the regime in which there is a LSS state in the absence of Ising coupling: $4t^2/U > T_K^{L/R}$, where $T_K^{L/R}$ is the Kondo temperature of the left or right pseudospin individually. Taking the leads to have a symmetric constant density of states, $\rho = 1/2D$, with half-band-width $D = 2$, we focus on the case $U = 3$, $\Gamma = 0.2$, and $t = 0.3$. $\beta = 1/T$ is the inverse temperature. As U' is varied [a horizontal scan in Fig. 1(b)], the gate potential is chosen such that $\epsilon_d = -(U + U')/2$, placing the dots right at the midpoint of the two electron regime.

Thermodynamics—As a first step toward distinguishing the different phases, we look at the local charge susceptibility $\chi_c^{\rm loc} \equiv \int_0^\beta \langle A(\tau)A(0)\rangle d\tau$, where $A \equiv n_{L+} + n_{R+} - n_{L-} - n_{R-}$ and $n_{i,s}$ is the charge density of the dot labeled i, s. Figure 2(a) shows $\chi_c^{\rm loc}$ as a function of temperature for different values of U'. The curves show three types of behavior. First, for small Ising coupling ($U' \leq 0.11$), $\chi_c^{\rm loc}$ is roughly constant at low T and has a peak at higher temperature. This is the LSS phase. The value of T at which $\chi_c^{\rm loc}$ peaks decreases as the energy spacing between the singlet $|S\rangle$ and doublet, $\{|++\rangle, |--\rangle\}$, decreases. Second, at the other extreme, for large Ising coupling ($U' \geq 0.15$), $\chi_c^{\rm loc}$ behaves as $1/T$ down to our lowest T. This is a clear signature of the CO phase in which the two charge states $|++\rangle$ and $|--\rangle$ are degenerate. Third, for intermediate values of U', $\chi_c^{\rm loc}$ becomes large and then either decreases slightly at our lowest T or saturates. This behavior can be produced by either a near degeneracy between the singlet and doublet states or by charge

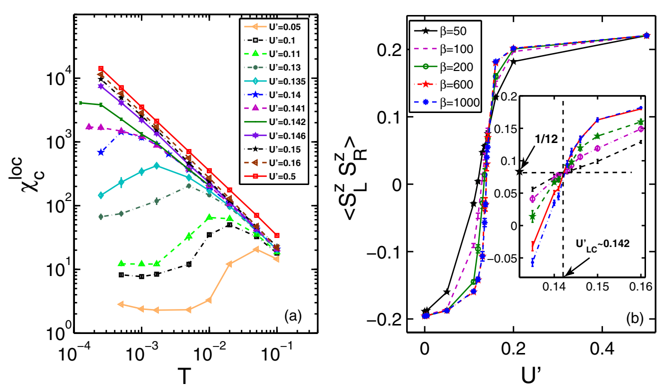

FIG. 2 (color online). (a) Local charge susceptibility as a function of temperature. The power-law behavior of the top three curves indicates the CO phase. The peak and low-T constants in the lowest curves indicate the LSS state. The low-T saturation of the middle curves is due to Kondo-like screening. (b) Pesudospin-pseudospin correlation as a function of U' for different β. Inset: Zoom near the crossing point. The crossing of the singlet and doublet levels occurs at $U'_{\rm LC} = 0.142$, corresponding to level crossing ($U = 3$, $\Gamma = 0.2$, and $t = 0.3$). The error bars are from statistical error.

Kondo screening of the doublet $\{|++\rangle, |--\rangle\}$. As we will see from the conductance data below, the QPT to the CO phase occurs at a value $U'_{\rm KT}$ between 0.146 and 0.15.

To extract the position of the level crossing between $|S\rangle$ and $\{|++\rangle, |--\rangle\}$, we calculate the pseudospin correlation function $\langle S^z_L S^z_R\rangle$ as a function of U' for different T [Fig. 2(b)], where $S^z_i = (\hat{n}_{i+} - \hat{n}_{i-})/2$. For $U' = 0$, the ground state is the LSS so that $\langle S^z_L S^z_R\rangle \simeq -0.2$ is close to $-1/4$. On the other hand, for large U', in the CO phase, $\langle S^z_L S^z_R\rangle$ is positive and approaches 1/4. (The charge fluctuations due to tunneling to the leads causes the values to differ slightly from $\pm 1/4$.) The crossing point of the curves for different temperatures gives the position of the (renormalized) level crossing. The inset shows that it occurs at $\langle S^z_L S^z_R\rangle \approx 1/12$, which is consistent with the isolated-dots limit. The position of the level crossing is, then, $U'_{\rm LC} \approx 0.142$; note that this does *not* coincide with the QPT to the CO phase ($0.146 < U'_{\rm KT} < 0.15$).

Conductance.—Conductance is a crucial observable experimentally. However, the QMC method is only able to provide numerical data for the imaginary time Green function at discrete Matsubara frequencies—the conductance cannot be directly calculated. The zero bias conductance for an impurity model can be obtained [15] by extrapolating to zero frequency. We have recently shown that this method works very well for Anderson-type impurity models in the Kondo region at low temperature [16].

We use this method [12] to find the conductance between the left and right leads as a function of U' for different T; the results are shown in Fig. 3. For U' small ($U' \lesssim 0.1$), the conductance is small because the phase shift is nearly zero in the LSS state [10]. For U' large ($U' > 0.15$), the conductance is also small and approaches zero as $U' \to \infty$, consistent with the argument in Ref. [8]. At intermediate values of U', there is a strikingly sharp conductance peak near the value of U' where the level crossing occurs. Here, the conductance increases as T decreases and approaches the unitary limit $2e^2/h$ as $T \to 0$. The position of the conductance peak approaches the level crossing $U' = 0.142$ at low temperature [12]. Its association with the level crossing suggests that this peak comes from fluctuations produced by the degeneracy of $|S\rangle$ and $\{|++\rangle, |--\rangle\}$.

A sharp jump appears after the peak: notice that the conductance at $U' = 0.146$ *increases* at lower temperature while that at 0.15 *decreases* [see Figs. 3(b) and 3(c) for clarity]. The latter behavior is the signature of the CO phase, while the former suggests a Kondo-like phase, namely, the dynamic screening of the $\{|++\rangle, |--\rangle\}$ doublet. Thus, this sharp jump is associated with the KT QPT from the screened to the CO phase [8], which occurs between $U' = 0.146$ and 0.15.

Effective theory near the level crossing.—To gain insight into the conductance peak, we develop an effective theory near the level crossing. Using Γ/U as a small parameter, we make a Schrieffer-Wolff transformation to integrate out $|T0\rangle$; to include tunneling, processes of order $\Gamma t/U^2$ must

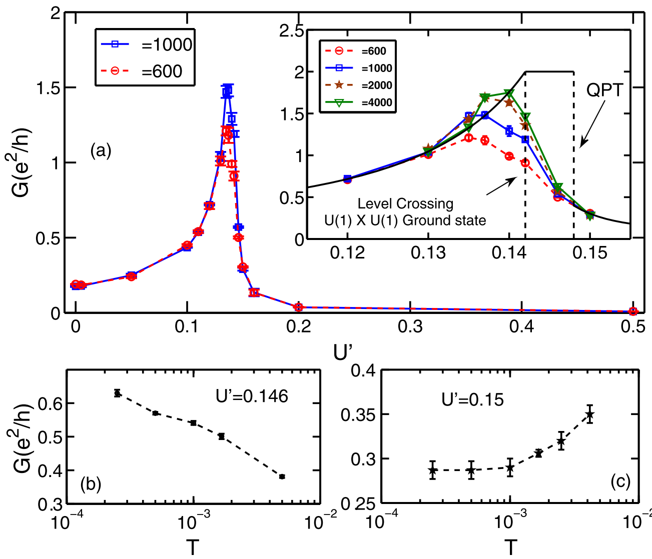

FIG. 3 (color online). (a) Zero bias conductance as a function of U' for two values of β. Inset: Zoom on the peak caused by the $U(1) \times U(1)$ ground state. The $T = 0$ expectation from the effective theory near the level crossing is indicated schematically by the black solid line; the two points of discontinuity (the level crossing and the KT QPT) are marked by dashed lines. (b), (c) Conductance as a function of temperature for $U' = 0.146$ and 0.15, respectively; the opposite trend in these two curves shows that they are on opposite sides of the QPT. The error bars are from both statistical and extrapolation error.

be included [17]. Higher-order terms in Γ/U are neglected. In the leads, only the combinations $\sum_k c^\dagger_{isk} \equiv c^\dagger_{0,is}$ need be considered as these are the locations to which the dots couple. The resulting effective Kondo Hamiltonian reads

$$H^{\rm eff}_{\rm Kondo} = J^{\rm I}_\perp (M^{\rm I}_+ S^{\rm I}_- + M^{\rm I}_- S^{\rm I}_+) + 2J^{\rm I}_z M^{\rm I}_z S^{\rm I}_z + J^{\rm II}_\perp (M^{\rm II}_+ S^{\rm II}_- + M^{\rm II}_- S^{\rm II}_+) + 2J^{\rm II}_z M^{\rm II}_z S^{\rm II}_z. \quad (3)$$

The definitions of pseudospins type I and II—the operators M act on the dots and the operators S act on the lead sites—are given in the supplementary material [12]. For $t/U \ll 1$ and particle-hole symmetry, $J^\perp_{\rm I} \simeq J^z_{\rm I} \simeq 4V^2/(U + U')$ and $J^\perp_{\rm II} \simeq J^z_{\rm II} \simeq 8V^2 t/(U + U')^2$.

Renormalization effects in $H^{\rm eff}_{\rm Kondo}$ can be analyzed using poor man's scaling [18], yielding the scaling equations

$$\begin{aligned} dJ^{\rm I}_\perp/d\ln D &= -2\rho(J^{\rm I}_\perp J^{\rm I}_z + 3J^{\rm II}_\perp J^{\rm II}_z) \\ dJ^{\rm II}_\perp/d\ln D &= -2\rho(J^{\rm II}_\perp J^{\rm I}_z + 3J^{\rm I}_\perp J^{\rm II}_z) \\ dJ^{\rm I}_z/d\ln D &= -2\rho[(J^{\rm I}_\perp)^2 + (J^{\rm II}_\perp)^2] \\ dJ^{\rm II}_z/d\ln D &= -4\rho J^{\rm I}_\perp J^{\rm II}_\perp. \end{aligned} \quad (4)$$

Numerical solution of these equations reveals that at a certain value of D all the coupling constants simultaneously diverge. This defines the problem's characteristic energy scale D_0, which can be considered the Kondo temperature at the level crossing, $T^{\rm LC}_K$. The coupling constants have a fixed ratio as they diverge: $\lim_{D\to D_0} J^{\rm I}_\perp : J^{\rm II}_\perp : J^{\rm I}_z : J^{\rm II}_z \to \sqrt{2} : \sqrt{2} : 1 : 1$, suggesting an emergent symmetry in the ground state.

Symmetry analysis.—The six S operators form an $SO(4)$ algebra [12]. However, the six M operators do not; rather they form part of an $SU(3)$ algebra—the missing operators are $|++\rangle\langle--|$ and $|--\rangle\langle++|$ [12]. Since $H^{\rm eff}_{\rm Kondo}$ is the product of two objects which generate different algebras, the symmetry of the system must be a subgroup of both $SO(4)$ and $SU(3)$. To study the complete symmetry group of both the bare and fixed-point Hamiltonians, consider the total z component of pseudospins type I and II, $S^{\rm I}_{z,\rm tot} \equiv M^{\rm I}_z + \sum_k S^{\rm I}_{z,k}$, $S^{\rm II}_{z,\rm tot} \equiv M^{\rm II}_z + \sum_k S^{\rm II}_{z,k}$. $S^{\rm I/II}_{z,k}$ is defined by replacing c_0 with c_k in the definition of $S^{\rm I/II}_z$. One can check that $[S^{\rm I}_{z,\rm tot}, H_{\rm lead} + H^{\rm eff}_{\rm Kondo}] = 0$, which gives a (pseudo)spin $U(1)$ symmetry for the bare Hamiltonian. The bare Hamiltonian also commutes with interchanging L and R or interchanging $+$ and $-$. Thus, the symmetry of the bare Hamiltonian is $U(1)_S \times Z_{2,LR} \times Z_{2,+-}$ [an irrelevant charge $U(1)$ is ignored].

At the fixed point, $\lim_{D\to D_0} J^{\rm I}_\perp / J^{\rm II}_\perp \to 1$ implies that both $S^{\rm I}_{z,\rm tot}$ and $S^{\rm II}_{z,\rm tot}$ commute with the Hamiltonian: there is an additional $U(1)$ symmetry. Furthermore, note that $\exp(i\theta S^{\rm II}_{z,\rm tot})$ generates the $L \leftrightarrow R$ transformation for $\theta = \pi$. Therefore, the $Z_{2,LR}$ symmetry of the bare Hamiltonian is enhanced, becoming an emergent $U(1)$ symmetry. The complete symmetry group at the fixed point (ground state) is $U(1)_S \times U(1)_{LR} \times Z_{2,+-}$, where the $Z_{2,+-}$ symmetry is irrelevant for the Kondo physics.

Experimental accessibility.—We address two main experimental issues: making of the system and sensitivity to symmetry of parameters. Because of the tunneling t, a small capacitive coupling U_h between dots in the horizontal direction will be present. However, the QPT and $U(1) \times U(1)$ state both still exist provided that $U' - U_h > U'_{\rm KT}$. This may be achieved by using floating metallic electrodes [19] or an air bridge [20] over the diagonal dots to boost U'. Experimentally, tuning through the transition will result from changing t rather than U' [i.e., a vertical cut in Fig. 1(b)]. When tuning t, U_h will be affected, but the change is small and can be neglected. We need $U \gg U'$ to exclude configurations involving both electrons on the left or right side; the total number of electrons in the four dots can be determined by higher temperature Coulomb blockade experiments.

Possible experimental observation is greatly aided by the fact that not all the symmetries are essential. Those involving the tunneling between the dots or the coupling to the leads, for instance, merely change the coupling constants in the effective Hamiltonian. In both cases, a renormalization-group analysis shows that the $U(1) \times U(1)$ strong-coupling fixed point remains stable. For the QPT, since the asymmetry of t_+ and t_- does not introduce a relevant operator, it does not affect the essential nature of the QPT.

For our scenario, the one crucial symmetry is that $|++\rangle$ and $|--\rangle$ be degenerate; this can be achieved by fine-tuning the gates controlling the levels in the dots. For the $U(1) \times U(1)$ state we need to have the three-level crossing (by varying one parameter) which gives rise to the effective Hamiltonian Eq. (3). If the detuning is smaller than $T^{\rm LC}_K$, the crossover is still sharp and the $U(1) \times U(1)$ state remains stable. For the QPT, the detuning $\delta\epsilon$ induces a relevant perturbation in the CO phase [9]. However, a sharp (but continuous) crossover does still occur in the conductance as long as $\delta\epsilon \ll T^{\rm LC}_K$ and $T \lesssim \delta\epsilon$ [9]. Note that observation of a charge Kondo (CK) effect separately in the left and right dots could be used to zero in on a small $\delta\epsilon$ because of the requirement $\delta\epsilon < T^{\rm CK}_K$.

We thank G. Finkelstein and A. M. Chang for useful discussions. This work was supported in part by the U.S. NSF Grant No. DMR-0506953.

[1] S. Sachdev, arXiv:0901.4103.
[2] R. Coldea *et al.*, Science **327**, 177 (2010).
[3] P. Coleman, arXiv:cond-mat/0206003.
[4] M. Grobis, I. G. Rau, R. M. Potok, and D. Goldhaber-Gordon, arXiv:cond-mat/0611480.
[5] A. M. Chang and J. C. Chen, Rep. Prog. Phys. **72**, 096501 (2009).
[6] T. Kuzmenko, K. Kikoin, and Y. Avishai, Phys. Rev. Lett. **89**, 156602 (2002); T. Kuzmenko, K. Kikoin, and Y. Avishai, Phys. Rev. B **69**, 195109 (2004).
[7] M. Vojta, Philos. Mag. **86**, 1807 (2006).
[8] M. Garst, S. Kehrein, T. Pruschke, A. Rosch, and M. Vojta, Phys. Rev. B **69**, 214413 (2004).
[9] M. R. Galpin, D. E. Logan, and H. R. Krishnamurthy, Phys. Rev. Lett. **94**, 186406 (2005); J. Phys. Condens. Matter **18**, 6545 (2006).
[10] I. Affleck, A. W. W. Ludwig, and B. A. Jones, Phys. Rev. B **52**, 9528 (1995), and references therein.
[11] G. Zaránd, C.-H. Chung, P. Simon, and M. Vojta, Phys. Rev. Lett. **97**, 166802 (2006), and references therein.
[12] See supplementary material at http://link.aps.org/supplemental/10.1103/PhysRevLett.105.256801 for text addressing (1) extracting the conductance from the QMC calculations, (2) the shape of the conductance peak, (3) more detail about the effective theory near the level crossing, and (4) an effective theory near the QPT.
[13] O. F. Syljuåsen and A. W. Sandvik, Phys. Rev. E **66**, 046701 (2002).
[14] J. Yoo, S. Chandrasekharan, R. K. Kaul, D. Ullmo, and H. U. Baranger, Phys. Rev. B **71**, 201309(R) (2005).
[15] O. F. Syljuåsen, Phys. Rev. Lett. **98**, 166401 (2007).
[16] D. E. Liu, S. Chandrasekharan, and H. U. Baranger, Phys. Rev. B **82**, 165447 (2010).
[17] Processes of order $\Gamma t^n/U^{n+1}$ produce the same terms in the effective Hamiltonian as Γ/U and $\Gamma t/U^2$ processes, and so do not lead to any essential difference.
[18] P. W. Anderson, J. Phys. C **3**, 2436 (1970).
[19] A. Hubel, J. Weis, W. Dietsche, and K. v. Klitzing, Appl. Phys. Lett. **91**, 102101 (2007).
[20] E. Girgis, J. Liu, and M. L. Benkhedar, Appl. Phys. Lett. **88**, 202103 (2006).